한국정밀공학회지 제 40 권 제 5 호 pp. 409-414 May 2023 / 409
J. Korean Soc. Precis. Eng., Vol. 40, No. 5, pp. 409-414 http://doi.org/10.7736/JKSPE.022.114
ISSN 1225-9071 (Print) / 2287-8769 (Online)

PCAS 공정으로 제조된 WC-5wt.%TiC 소결체의 극저온처리 효과

Study of Cryogenic Treatment Effects on WC-5wt.%TiC Compact Fabricated by PCAS

이정한[1], 박범순[1], 박현국[1], 박재철[1,#]
Jeong Han Lee[1], Bum Soon Park[1], Hyun Kuk Park[1], and Jae-Cheol Park[1,#]

1 한국생산기술연구원 동력소재부품연구그룹 (Automotive Materials and Components R&D Group, Korea Institute of Industrial Technology)
Corresponding Author / E-mail: jerwual@kitech.re.kr, TEL: +82-62-600-6182)
ORCID: 0000-0003-3615-3933

KEYWORDS: Pulsed current activated sintering (펄스전류 활성화 소결), Tungsten carbide (텅스텐 카바이드), Titanium carbide (티타늄 카바이드), Cryogenic treatment (극저온 처리), Hard materials (고강도 소재)

The WC-5wt.% TiC compacts, which was fabricated by pulsed current activated sintering process (PCAS), were cryogenically treated to improve the mechanical performance. The densely consolidated specimens were exposed to liquid nitrogen for 6, 12, and 24 h. All cryogenically treated samples exhibited compressive stress in the sintered body compared with the untreated sample. The cryogenically treated samples exhibited significant improvement in mechanical properties, with a 9% increase in Vickers hardness and a 52.6% decrease in the fracture toughness compared with the untreated samples. However, excessive treatment of over 12 h deteriorates the mechanical properties due to tensile stress in the specimens. Therefore, the cryogenic treatment time should be controlled precisely to obtain mechanically enhanced hard materials.

Manuscript received: September 27, 2022 / Revised: December 22, 2022 / Accepted: March 6, 2023

NOMENCLATURE

V	=	Voltage
A	=	Ampere
ε	=	Densification Strain
m	=	Sintering Exponent
τ	=	Crystallite Size
K	=	Shape Factor
λ	=	X-ray Wavelength
β	=	Full Width at Half Maximum
θ	=	Bragg Angle
H_v	=	Vickers Hardness
K_{IC}	=	Fracture Toughness
f	=	Gravity Force
H	=	Hardness
P	=	Applied Load
E	=	Elastic Modulus
C	=	Length of Crack Propagation

1. Introduction

Tungsten carbide (WC), which contains cemented carbides, has attracted considerable attention owing to its high hardness, high elastic modulus, and wear resistance properties [1]. Cobalt, a typical binder material, improves the wettability of conventional cemented carbides and possess excellent sintering properties [2,3]. However, cobalt materials face certain disadvantages, including

high cost and environmental pollution; thus, a new metal binder is required to replace them. In recent years, several studies have been conducted to develop new hard materials using various cemented carbides, such as VC, Cr_3C_2, TiC, TaC, and NbC [4-6].

Composites sintered with WC-based cemented carbide materials can be strengthened not only by alloying but also by heat and cryogenic treatments. In particular, deep cryogenic treatment could have tremendous benefits, such as mitigating the thermal shock of materials, improving wear resistance, and extending tool life. Recently, several studies based on cryogenic treatment have been reported to significantly improve mechanical properties, such as hardness, compression strength, fatigue resistance, and wear resistance [7]. Kalsi et al. [8] reported that cryogenically treated tungsten carbide tools improved the flank wear resistance, thereby providing a better surface finish. Similarly, Yan et al. [9] observed an increase in the hardness and wear resistance of cryogenically treated tungsten carbide inserts. In addition, Yong and Ding [10] proved that cryogenic treatment improves the compressive as well as fatigue strength of cemented carbide tools without affecting their toughness and bending strength.

Therefore, the cryogenically treated WC-based cemented carbide improves the mechanical strength of the materials. However, studies have revealed that crystallographic changes in materials with cryogenic treatment time can have negative and positive effects on their mechanical performance. Therefore, in this study, the correlation between the crystallinity and mechanical strength of the WC-5wt.% TiC fabricated with different cryogenic treatment times was investigated.

2. Experimental Details

WC powder (W: 94.0 wt.% and C: 6.0 wt.%, ≤ 0.5 μm, TaeguTec Ltd.), which has 99.9% purity and an average particle size of 0.5 μm, was used as the starting material. Titanium carbide (TiC) powder (Alfa Aesar) with a purity of 99.5% and average particle size of 10 μm was used as an additive material. The WC-TiC mixed powders with a composition ratio of 95:5 wt.% were fabricated using a high-energy ball mill (Pulverisette5, FRITSCH Ltd.) at 250 RPM for 10 h. WC compacts with a 5 wt.% TiC were fabricated using a pulsed current activated sintering (PCAS) system, including the 25 V and 1,000 A of DC power supply. First, the PCAS system was evacuated at a base pressure of 10^{-3} Pa, and subsequently, a uniaxial pressure of 60 MPa was applied. The heating rate was approximately 2°C/sec during the entire process, and natural cooling was performed until the temperature of the sintered body decreased to room temperature. Furthermore, the naturally cooled compact was cryogenically treated as direct contact between the cryogen and the samples. Liquid nitrogen was used as the cryogen, which allowed the ambient temperature of the sample to drop to -196°C. The structural and mechanical properties of WC-5 wt.% TiC compact, cryogenically treated in liquid nitrogen for 6, 12, and 24 h, were investigated in detail.

To confirm the microstructure of the sintered body, the cryogenically treated or untreated specimens were etched at room temperature for 30 s using a Murakami solution. This reagent was stirred for 3 min after mixing 10 g NaOH powder and 10 g potassium ferricyanide ($K_3Fe(CN)_6$) in 100 ml distilled water. The surface morphologies of the etched specimens were examined using field-emission scanning electron microscopy (FE-SEM, Quanta 200). In addition, the crystallinity of the sintered body was analyzed using X-ray diffraction (XRD, PANalytical X'pert MPD), and the Vickers hardness test was used to analyze the mechanical properties of the WC-5 wt.% TiC hard materials.

3. Results and Discussion

Fig. 1(a) shows variations in the sintering temperature and shrinkage displacement of WC-5 wt.% TiC compact as a function of sintering time. As shown in Fig. 1(a), the WC-5 wt.% TiC compact had three distinguishable inflection points in terms of shrinkage displacement. The critical points were divided into three regions at specific temperatures: Stage I (550-683°C), Stage II (683-864°C), and Stage III (864-1,081°C). Stage I is the initial stage of sintering, which represents the region in which the particle movement by thermal expansion forms a neck. The sintering properties are determined in stage II, where the grain growth and densification processes occur. The final densification region represented by Stage 3 involves the removal of closed pores caused by grain growth, diffusion, and plastic deformation of WC-5 wt.% TiC. After completion of the sintering process, WC-5 wt.% TiC sample had a relative density of 99.3%, thus confirming that the densification process was totally completed.

Densification can be inferred from the sintering exponent derived from the shrinkage displacement and sintering temperature. The sintering exponents were calculated using Eq. (1) [11], which can also be expressed as a logarithmic function:

$$\ln(\varepsilon) = (1/m)\ln(K/T) + (1/m)\ln(t) \quad (1)$$

The sintering exponents can be defined using the slope of the shrinkage strain vs. temperature plot, as shown in Fig. 1(b). The WC-5 wt.% TiC sample had two densification zones. In zone 1,

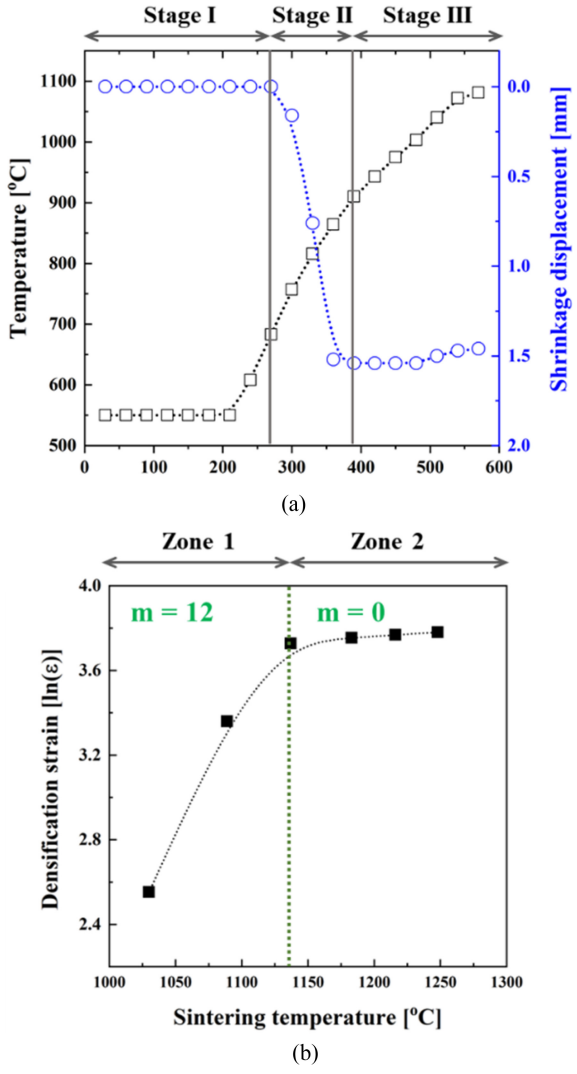

Fig. 1 (a) Temperature and shrinkage displacement of WC-5 wt.% TiC sample as a function of sintering time. (b) Variations in densification strain in the shrinkage zone

rapid densification occurs in the macro area. On the contrary, in zone 2, densification proceeds as open pores inside the sintered body are removed. Since the densification strain is defined only in the section where the change in shrinkage length is observed, the sintering exponent (m = 12) of the WC-5 wt.% TiC sintered was obtained as shown in Fig. 1(b).

Fig. 2 shows the surface morphologies of WC powder, TiC powder, WC-5 wt.% TiC compact and cryogenically treated WC-5wt.% TiC samples. Fig. 2(a) shows surface morphology of the WC powder, which is the starting material of the WC-5wt.% TiC compact, and has the average particle size below 500 nm. As shown in Fig. 2(b), TiC power as an additive material, has the randomly distributed morphology with the average grain size below 10 μm. The WC-5 wt.% TiC sintered compact prepared with the above two powders showed a densely packed micro-

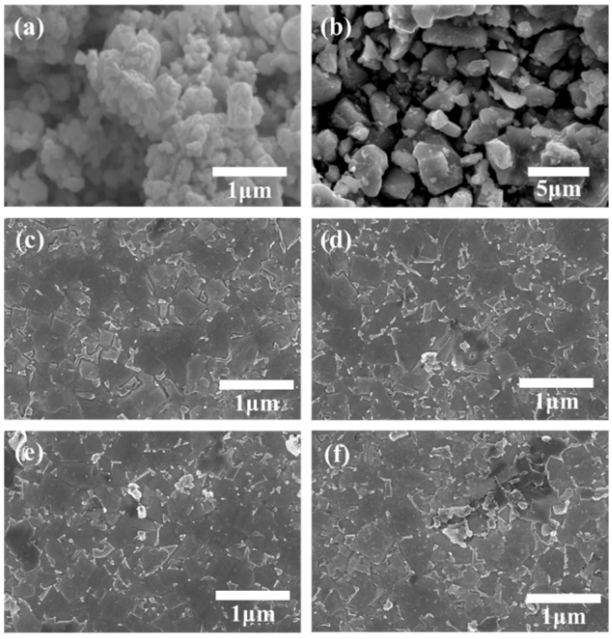

Fig. 2 Surface morphologies of (a) WC powder and (b) TiC powder. The surface images of WC-5 wt.% TiC compacts as a function of cryogenic treatment time: (c) untreated, (d) 6 h, (e) 12 h, and (f) 24 h

structure without pores, and the average grain size of the sintered compact had a value of 487 nm. The WC-5 wt.% TiC compact had a grain size similar to that of WC starting materials, which indicates that grain growth was considerably suppressed during the densification process. Samples (d)-(f) that were cryogenically treated for 6, 12, and 24, respectively, showed the similar morphology to that of the non-cryogenic treated samples. This means that the cryogenically treated compacts were not deformed by thermal shock; Therefore, it is necessary to further investigate the effect of the cryogenic treatment on the sintered body by clarifying the correlation between crystallinity and mechanical strength.

Figure 3(a) shows XRD patterns of cryogenically treated and untreated WC-5 wt.% TiC samples depending on the dipping time. In all cryogenically treated samples, only diffraction planes corresponding to hexagonal structures were observed, indicating that no secondary phases such as carbon or TiC additives were observed. As shown in Fig. 3(b), the diffraction peaks exhibited by all the cryogenically treated samples shifted to higher angles compared to the untreated samples. According to the Bragg's law, the diffraction angle and lattice constant are inversely proportional; hence, compressive strength can be inferred to exist in the cryogenically treated samples. However, in case of cryogenically treated samples, it was observed that the diffraction peaks gradually shifted to lower angles as the cryogenic treatment time increased. Furthermore, crystallite sizes of WC-5 wt.% TiC

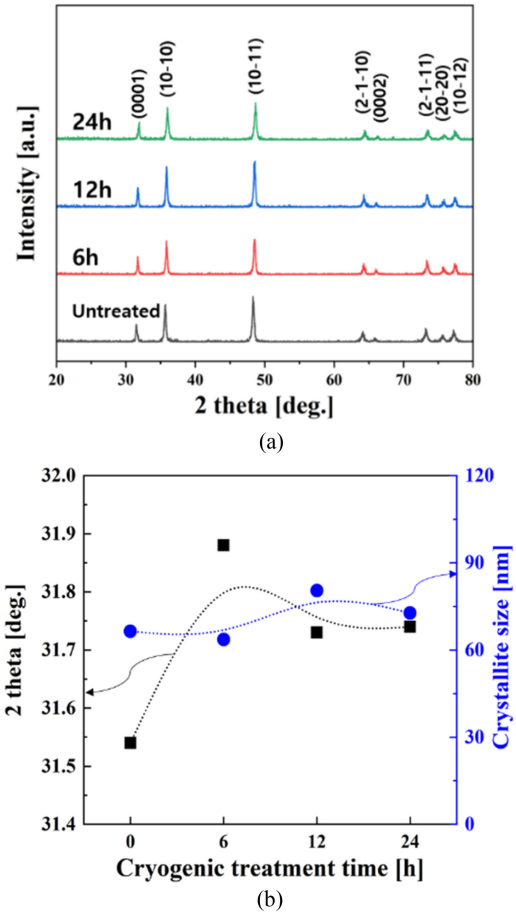

Fig. 3 (a) XRD patterns of WC-5 wt.% TiC samples as a function of cryogenic treatment time. (b) diffraction peak positions and crystallite sizes corresponding to (0001) diffraction plane

Table 1 Variations in Vickers hardness and fracture toughness as a function of cryogenic treatment time

Cryogenic treatment time [h]	H_v [kg/mm^2]	K_{IC} [MPa*m$^{0.5}$]
0	1,821.4±21.3	17.1±0.3
6	2,044.9±22.3	11.3±0.2
12	1,951.6±21.9	9.8±0.2
24	1,956.1±23.2	9.0±0.2

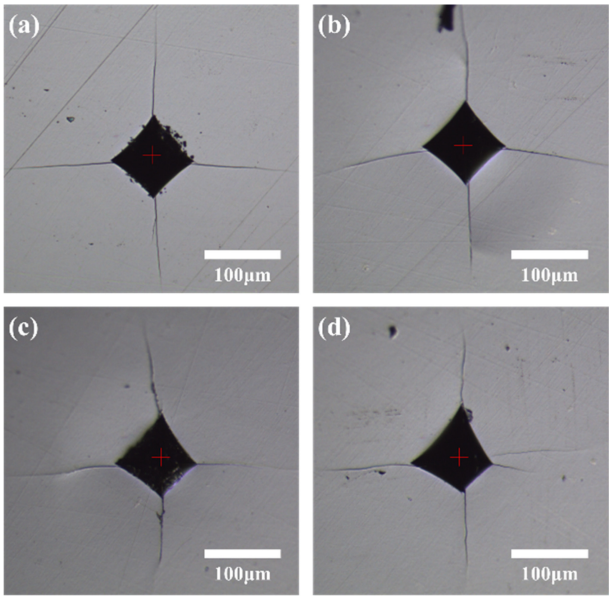

Fig. 4 Microstructure images with hardness indentations of WC-5 wt.% TiC sintered bodies according to the cryogenic treatment time: (a) 0 h, (b) 6 h, (c) 12 h, (d) 24 h

samples were calculated using the Scherrer equation ($\tau = K\lambda/\beta\cos\theta$). The crystallite size of WC-5 wt.% TiC samples were 66.5, 63.6, 80.4, 72.7 nm, respectively, as increasing cryogenic treatment times, showing that no remarkable changes are observed regardless of the cryogenic treatment times. The XRD results revealed that the cryogenic treatment of WC-5 wt.% TiC sample developed compressive stress in the sintered body, which significantly improved its mechanical properties. However, tensile stress was weakly expressed in the sintered body with a gradual increase in the cryogenic treatment time, thereby leading to a decrease in the mechanical strength of the sintered body. Therefore, the sintered body must be strengthened via proper cryogenic treatment conditions.

To examine the effect of cryogenic treatment on the mechanical properties of the sintered body, variations in Vickers hardness and fracture toughness according to the cryogenic treatment time are presented in Table 1. The hardness and fracture toughness were determined through indentation cracking with a load of 10 kgf. In addition, fracture toughness (K_{IC}) obtained from the crack propagation lengths in the four directions of the indentations were used to determine the cracking resistance, which was calculated by the Antis formula [12].

$$K_{IC} = 0.016(E/H)^{1/2}P/C^{3/2} \quad (2)$$

where E is the elastic modulus, H is the hardness, P is the applied load, and C is the length of crack propagation.

The untreated sample exhibited Vickers hardness of 1,821.44±21.3 kg/mm^2 and fracture toughness of 17.1±0.3 MPa*m$^{0.5}$. In contrast, all the cryogenically treated samples exhibited an average Vickers hardness of 1,984.2±22.8 kg/mm^2, which was approximately 9% higher than that of the untreated sample. Furthermore, the fracture toughness of the cryogenically treated sample exhibited a decrease of more than 52.6% compared to the non-cryogenically treated sample, thus verifying that the mechanical properties were dramatically improved. The mechanical properties were closely related to the XRD results; in particular, the compressive and tensile stresses in the sintered body had a significant effect on mechanical strength. The XRD results

revealed that the cryogenically treated sample had excellent crystallinity compared with the untreated sample, which resulted in low crystallographic defects in the sintered body. Additionally, the XRD results of the cryogenically treated sample exhibited improved mechanical strength owing to the occurrence of compressive stress in the sintered body. Although it was confirmed that cryogenic treatment could have a positive effect on improving mechanical properties, a gradual decrease in Vickers hardness was observed as the cryogenic treatment time increased. This is believed that the TiC additives at the WC/TiC interface promote the grain growth biased toward the basal facet, which has relatively low energy during cryogenic treatment. As shown in Fig. 3(b), it can be confirmed that the crystallite size of samples cryogenically treated over 12 h increases, and this increase in crystallite sizes eventually leads to the deterioration in mechanical properties. Consequently, the results verified that the compressive stress formed in the sintered body through cryogenic treatment significantly contributed to the improvement of the Vickers hardness and rupture strength. Nonetheless, note that excessive cryogenic treatment may degrade the crystallinity and decrease the mechanical strength of the sintered body; therefore, precise control of the cryogenic treatment time is necessary.

4. Conclusions

The effects of cryogenic treatment in improving the mechanical properties of WC-5 wt.% TiC hard materials were studied in detail. Compressive stress in the sintered body emerged with increasing cryogenic treatment time owing to the decrease in the lattice constant. Regardless of the deep cryogenic treatment time, none of the samples showed phase changes, precipitation, or secondary phases in the specimens. However, the sample treated over 12 h revealed tensile stress, which resulted in degradation of the mechanical strength. As a result, it has been demonstrated that cryogenic treatment can have a beneficial effect on tool hardening as well as degrade performance with treatment time.

ACKNOWLEDGEMENT

This study has been conducted with the support of the Korea Institute of Industrial Technology as “Development of core technologies of AI based self-power generation and charging for next-generation mobility (KITECH EH-23-133)”.

REFERENCES

1. Hur, M. G., Shin, M. K., Kim, D. J., Yoon, D. H., (2018), Defect control of the WC hardmetal by mixing recycled WC nano powder and tungsten powder, Metals and Materials International, 24(4), 301-305.
2. Viswanathan, V., Agarwal, A., Ocelik, V., De Hosson, J., Sobczak, N., Seal, S., (2006), High energy density processing of a free form Nickel-alumina nanocomposite, Journal of Nanoscience and Nanotechnology, 6(3), 651-660.
3. Liu, G., Guo, S., Li, J., Chen, K., Fan, D., (2017), Fabrication of hard cermets by in-situ synthesis and infiltration of metal melts into WC powder compacts, Journal of Asian Ceramic Societies, 5(4), 418-421.
4. Huang, S., Liu, R., Li, L., Van der Biest, O., Vleugels, J., (2008), NbC as grain growth inhibitor and carbide in WC-Co hardmetals, International Journal of Refractory Metals and Hard Materials, 26(5), 389-395.
5. Huang, S., Li, L., Vanmeensel, K., Van der Biest, O., Vleugels, J., (2007), VC, Cr3C2 and NbC doped WC-Co cemented carbides prepared by pulsed electric current sintering, International Journal of Refractory Metals and Hard Materials, 25(5-6), 417-422.
6. Lauter, L., Hochenauer, R., Buchegger, C., Bohn, M., Lengauer, W., (2016), Solid-state solubilities of grain-growth inhibitors in WC-Co and WC-MC-Co hardmetals, Journal of Alloys and Compounds, 675, 407-415.
7. Kaya, E., Ulutan, M., (2017), Tribological and mechanical properties of deep cryogenically treated medium carbon micro alloy steel, Metals and Materials International, 23(4), 691-698.
8. Kalsi, N. S., Sehgal, R., Sharma, V. S., (2012), Comparative study to analyze the effect of tempering during cryogenic treatment of tungsten carbide tools in turning, Advanced Materials Research, 410, 267-270.
9. Yan, H., Xu, H., Luo, X., (2010), The research on process of deep cryogenic treatment for YT15 carbide insert, Proceedings of the 2010 International Conference on Machine Vision and Human-Machine Interface, 725-728.
10. Yong, J., Ding, C., (2011), Effect of cryogenic treatment on WC-Co cemented carbides, Materials Science and Engineering: A, 528(3), 1735-1739.
11. Lee, J.-H., Oh, I.-H., Kim, J.-H., Hong, S.-K., Park, H.-K., (2021), Rapid consolidation of WC-ZrSiO 4 hard materials by spark plasma sintering: Microstructure, densification, and mechanical properties, Metals and Materials International, 27, 3409-3416.
12. Dukino, R. D., Swain, M. V., (1992), Comparative measurement of indentation fracture toughness with Berkovich and Vickers indenters, Journal of the American Ceramic Society, 75(12), 3299-3304.

Jeong Han Lee
Ph.D. in the Automotive Materials and Components R&D Group, Korea Institute of Industrial Technology.
E-mail: ljh88@kitech.re.kr

Bum Soon Park
M.D. candidate in the Automotive Materials and Components R&D Group, Korea Institute of Industrial Technology.
E-mail: bsbspark@kitech.re.kr

Hyun Kuk Park
Ph.D. in the Automotive Materials and Components R&D Group, Korea Institute of Industrial Technology.
E-mail: hk-park@kitech.re.kr

Jae Cheol Park
Ph.D. in the Automotive Materials and Components R&D Group, Korea Institute of Industrial Technology.
E-mail: jerwual@kitech.re.kr